Thermomechanical Properties Optimisation of Selected Ceramic Materials

Abayomi Cyril Ogundola[*1,2]; Olufemi Olusegun Ajide[1]; Temidayo Emmanuel Omoniyi[4]; Emmanuel Tunde Daodu[2,3]; Ayodeji Olaoluwa Alake[2]; Johnson Oluwasegun Ikare[2,3]; Sheriff Olamide Olowo[2]; Odunayo Peter Aminu[2]

[1]Department of Mechanical Engineering, University of Ibadan, Ibadan, Nigeria
[2]National Space Research and Development Agency NASRDA, Abuja, Nigeria
[3]Department of Mathematics, Federal University of Technology, Akure, Nigeria
[4]Department of Wood Products Engineering, University of Ibadan, Ibadan, Nigeria

[*1,2]ORCID https://orcid.org/0009-0009-6505-9162

Corresponding Author: Abayomi Cyril Ogundola[*1,2]

Publication Date: 2026/09/19

Abstract: Ceramics are widely utilized to provide thermal and electrical insulation and are becoming significant structural materials in engineering industry. Researcher has reported on number of problems, such as surface deformation that resulted in crack propagation on the materials' surface under temperature loading. Hitherto, there is dearth of information on the establishment of a compressive stress field, which stops further crack propagation as one of the mechanisms of phase change. An advanced multistep multidimensional computational model was created on the commercially available Ansys finite-element platform to examine the thermomechanical properties of a few selected ceramic materials (alumina, silicon carbide, and chromium carbide) through surface respond. The computational model integrated the thermo-mechanic coupling, heat transfer and structural mechanics to forecast and assess not only the temperature field, crack propagation, but also phase change on the surface of the materials. However, in contrast to alumina and chromium carbide, silicon carbide has a higher safety factor, according to the study. In comparison to chromium carbide and alumina, which have respective minimum factors of safety of 0.42729 and 0.064329, silicon carbide has a minimum safety factor of 2.8125. According to the findings, there was a noticeable rise in thermal stress in the area closest to the chromium carbide geometry's outside. Additionally, it was noted that at 1800^0C, the thermal strain result shows that Alumina has a value of 0.0237 m/m, Silicon carbide has 0.0103 m/m, and Chromium carbide has 0.0124 m/m. This implies that silicon carbide has lowest thermal stress than the rest and silicon carbide exhibited few isolated cracks on the surfaces of geometry with the shears stress of 2.393x10^9 maximum at 1700^0C. According to the aforementioned findings, silicon carbide displayed compressive stress field lower than alumina and chromium carbide at temperatures higher than1800^0C.

Keywords: *Ceramic Materials, Alumina, Silicon Carbide, Chromium Carbide.*

How to Cite: Abayomi Cyril Ogundola; Olufemi Olusegun Ajide; Temidayo Emmanuel Omoniyi; Emmanuel Tunde Daodu; Ayodeji Olaoluwa Alake; Johnson Oluwasegun Ikare; Sheriff Olamide Olowo; Odunayo Peter Aminu (2026) Thermomechanical Properties Optimisation of Selected Ceramic Materials. *International Journal of Innovative Science and Research Technology*, 11(9), 474-483. https://doi.org/10.38124/ijisrt/26sep160

I. INTRODUCTION

Ceramics are widely utilized to provide thermal and electrical insulation and are becoming significant structural materials, even if metals still predominate in engineering applications [1, 2]. Ceramic has numerous uses in industries like the aerospace industry (rocket engine nozzle and gas turbines), furnaces (refractory lining), and automobiles (brake pads), due to their good mechanical properties like high thermal shock, high temperature resistance and thermal conductivity [3, 4]. A number of problems, such as surface deformation that resulted in crack propagation on the materials' surface under temperature loading [5, 6], limit the usage of ceramic materials in severe environments. Understanding how ceramic materials react to high-temperature, high-velocity impacts has recently attracted a lot of attention. Thus, one of the mechanisms of phase transformation that the researcher was unable to explain prior to a fracture tip propagation is the production of a compressive stress field, which inhibits further crack propagation during temperature loading [7, 8].

However, a lot of research has been done to examine how crack formation and deformation during temperature loading in ceramic materials. Zhang et al., and Sap et al., [9, 10] investigated the ceramic cracks caused by grinding and used three destructive examination techniques to characterise the cracks. The damage mechanism in silicon carbide ceramics (SiC) grinding was examined by Agarwal and Agarwal [7, 11,]. Engineering ceramics' surface microcracks were examined by Holmqust and Johnson [12]. They all came to the conclusion that, for ceramic materials with both brittle and ductile removal states, the facture toughness is crucial in determining the maximum depth of ductile cutting without microcrack. A brittle-to-ductile transition formula was developed by Wei and Sharma [13, 14], where the threshold value is inversely related to the material's static fracture toughness. Kurzawa and Hutzler [15, 16] devised a formula for the transition from brittle to ductile in which the threshold value depends on the material's static fracture toughness and other mechanical properties. Another important problem is the oxidation of materials made of ceramic composites during sintering or when they are put under high temperature strains of more than 1000 °C [17, 18].

Also, Timothy [19, 20] and Ross [21] also seek to understand the development of microcracks under impact loading. Experiments using repeating compressive loads and repeated hits illustrate the microscopic cracking process. Layered composites were detailed by [22, 23, 24] under dynamic load; the loading models show ongoing changes to the material. The internal structure alterations include grain rotations, maxima of plastic strain in metallic binders, and the emergence of microcracks [25, 26]. In their investigation of the fracture initiation mechanism for the ductile failure of the Co intergranular thin layer by [27] it was shown that the coalescence of micro-voids also contributes to the nucleation and spread of cracks. It has been discovered that the interfaces play a crucial role and that, depending on the phenomena in the interfaces, different modes of crack progression may be triggered. In this scenario, the nucleated fractures have the option of being temporarily stopped or of moving forward along the rigid bound barrier. However, there is still a void in the extensive research on WC/Co behavior in effects. The evaluation of analogous mechanical constants for ceramic materials under static load hasn't been done much up to this point.

The literature analysis demonstrates that one of the mechanisms of phase change that the researcher is interested in is the production of a compressive stress field that stops further crack propagation. Additionally, this computational model integrated the thermo-mechanic coupling, heat transfer, fluid flow, and structural mechanics to forecast and assess not only the temperature field, fluid flow, and resulting surface topography, but also the corresponding thermal stresses at high temperatures. Although the authors are aware that experimentally measured thermal properties of ceramic materials can also be useful to validate the theoretical prediction, no attempts were made to explore any experimental techniques due to the limitations mentioned above, including but not limited to material interaction and difficulties associated with preparing the surface of these brittle and hard structural ceramics.

II. MATERIALS AND METHODS

By varying the temperature range and examining the mechanical properties, the model's optimization has been carried out in this research project. Three ceramic-based composite materials' geometries (Alumina, Silicon Carbide, and Chromium Carbide) were modelled and studied. Utilizing the surface response approach, the produced 3-D model was loaded into the ANSYS CFD software, where heat flow analysis was carried out on ceramic base composite materials. By doing fluid flow analysis of ceramic base materials for inlet velocity and inlet temperature with boundary conditions, temperatures at the outlet are examined.

➢ *Conceptual Design*

- Ceramic Materials Geometry (CMG): To assess thermal stresses during temperature loading, an improved multiphysics computer model was created in the current work. The current efforts also concentrated on a connection between the thermomechanical qualities predicted and their correlation with the data generated by experiments. Although very significant authors reported on mechanism, causes of fracture, microcracking and deformation during thermal loading. The many physical characteristics of ceramic and metallic materials are displayed in Table 1. A geometry tube with an inner diameter of 0.1 meters and a length of 2.5 meters was created using CAD software with both ends are fixed, as shown in Figure 1. Calculating the properties of ceramic materials required determining the constant mechanical properties at initials condition shows by Table 1.

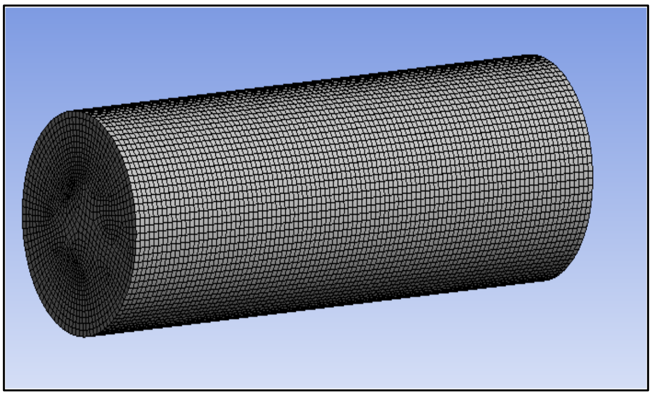

Fig 1 Meshing of Cylindrical Shape Under Thermal Conditions

ANSYS ICEM CFD software were used to simulate the geometry with a variety of materials and the temperature range at which the materials may fail.

ISSN No:-2456-2165 https://doi.org/10.38124/ijisrt/26sep160

Table 1 Phycio-Mechanical Properties of Ceramic Materials [28, 29]

Materials	Mechanical properties	Parameters/units
Al_2O_3 (Ceramics)	Density Thermal Conductivity Specific Heat Conductivity Poison's Ratio Elastic Limit Melting Point	$3.98mg/m^3$ 38.5W/m.k 955j/kg.k 0.33 665MPa 3638.93k
SiC (Ceramics)	Density Thermal Conductivity Specific Heat Conductivity Poison's Ratio Tensile strength Melting Point	$3217kg/m^3$ 350w/mk 1.09j/mol 0.192 0.1379GPa 2730^0C
Chromium Carbide (Ceramic)	Density Thermal Conductivity Specific Heat Conductivity Poison's Ratio Comprehensive strength Melting Point	$7.2mg/m^3$ 94W/m.k 520j/kg.k 0.22 430MPa 2150k

➢ *The Simulation Approach*

Thus, with appropriate boundary conditions set, the particle size, volume fraction, thermal conductivities of the ceramic-based composite materials, and temperature are taken into account. The solver was developed using ANSYS FLUENT's finite volume methodology. The mechanical properties of the ceramic-based metal composite materials (CM) were then predicted using a numerical Representative Volume Element (RVE) model, which integrated the governing equations across the entire control system.

➢ *Boundary Conditions*

Different boundary types that correspond with the physical circumstances are included with the ANSYS Fluent software. The body of the tube has thermal conditions with a starting temperature assumption of room temperature ranging to $\mathbf{1800^0C}$, and the two faces of the geometry were fixed supports. A boundary model that leverages "VELOCITY INLET" boundary types for fluid inlet has been implemented.

- *At the tube inlet (X=0)*

$V_x = V_o, V_r = 0$

- *At the outlect (X-L)*

Zero diffusion flux in the axial direction with mass balance correction.

- *Temperature Difference*

$T/_{r=R} = T_1$

$T/_{x=o} = T_o$

ube inlet temperature assumed to be Room temperature Ro,

At outlet

$T/_{x=0} = 0 \quad T_1$

➢ *Selective Governing Equation*

Based on the theory of continuum mechanics, the fundamental constitutive equations for composite materials, including the linear elasticity, strain-stress tensor, thermal stress, and the associated radial return evolution, were obtained [30, 25]. For Thermal stress.

L=L0

L=L0 (1+∝)

F/A=Y(L-L0)/L0

Y= Young's modulus of the materials

The actual expansion =Expansion due to rise in temperature

$$\delta = \alpha TL - \sigma$$

Actual strain= $\frac{\text{Actual expansion}}{\text{Original Length}}$

$=\frac{\alpha TL-\sigma}{L}$

Actual stress= $\frac{\alpha TL-\sigma}{L} X \in$

$OR \ \frac{\Delta L}{L} = \alpha L \nabla T$

Where,

$\Delta L = \text{change in Length}, L = \text{original Length},$

$\alpha = \text{linear coefficient of thermal expansion}$

$\in$= surface emissivity of the materials.

ISSN No:-2456-2165 https://doi.org/10.38124/ijisrt/26sep160

The constituent elements of the interface state's constitutive law state that: elastic modulus normal to the mid surface of the interface element (*n*) is 2.1x1011 Pa, both shear moduli in the directions that are tangent to the mid surface of the interface element (*s*, *t*) read 1.373x1011 Pa. The damage initiation condition is postulated quadratic.

$$\left\{\frac{\varepsilon_n}{\varepsilon_n^0}\right\}^2 + \left\{\frac{\varepsilon_s}{\varepsilon_s^0}\right\}^2 + \left\{\frac{\varepsilon_t}{\varepsilon_t^0}\right\}^2 = 1$$

$\varepsilon_n^0, \varepsilon_s^0, \varepsilon_t^0$ are maximum strain, ε_n is normal strain and $\varepsilon_{s,}\varepsilon_t$ are the two orthogonal (s) and (t) tangent directions to the interface element [26, 31].

Surface Tension

$(\mu) \times \left[\frac{\partial_y\,\partial T}{\partial T\,\partial x}\right]$, $(v) \times \left[\frac{\partial_y\,\partial T}{\partial T\,\partial y}\right]$, $(w) \times \left[\frac{\partial_y\,\partial T}{\partial T\,\partial z}\right]$ ------------ [32, 33, 34].

Radiation heat flux equation

$P = \epsilon \times \sigma \times A \times (T_2^4 - T_1^4)$,

$P = \text{Power dissipated through radiation}$

$\epsilon = \text{Surface emissivity of the materials}$

$\sigma = \text{Stefan} - \text{Boltzman constant } (5.67 \times 10^{-8} \text{W.M}^{-2}/\text{k}^{-4}$

$A = \text{Surface area}$

T_2 and T_1 = are surface temperature and ambient temperature respectively

Stress tensor $\nabla\mu 2 = \frac{du2}{dx}$, $\nabla u2 = \nabla\mu 2 \cong 1$,

$$\text{therefore } \varepsilon = {}^1/_2\,[\nabla u2 + (\nabla u2)^T]$$

Stress tensor $\sigma = s$

$s = s_0 + C: (\varepsilon - \varepsilon_0 - \varepsilon_{th})$........... [35],

➢ *Flow Chart*

As was already mentioned, boundary conditions were transformed using the finite difference method and a constitutive controlling equation was applied. The temperature range was stimulated using Ansy program.

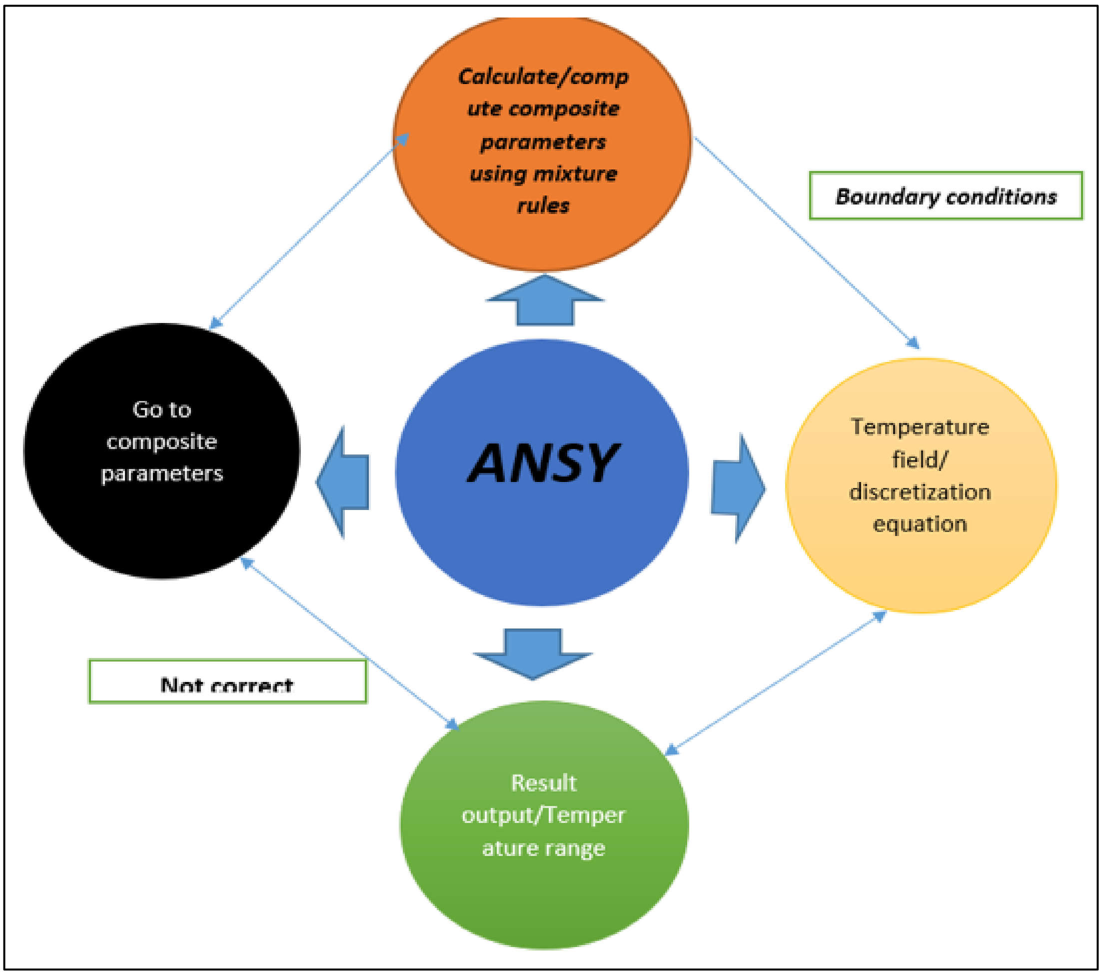

Fig 2 Overview of the Mathematical Added to the Existing Solver to Capture the Flow, Heat Transfer and Mechanical Properties of the Materials.

ISSN No:-2456-2165 https://doi.org/10.38124/ijisrt/26sep160

III. RESULT AND DISCUSSION

Study the three ceramic-based materials' microcracking processes in (figure 3). It was found that in all three ceramic materials optimized, the cracking process spreads evenly into the interfaces system. It was discovered that phase deformation is how heat stresses start cracking. As a result, both instantaneous and metastable phase deformation have all of the components present in total deformation in materials. Deformation toughening, as seen in figure 3b, is the reduction of a material's fracture toughness as a result of a phase shift that takes place at the crack tip. The adoption of ceramic materials for thermal applications was increased as a result of the capacity to show effective transformation toughening. Mamivand and Gosselet [34, 35] made an attempt at modeling to show how zirconia ceramic based materials undergo transition toughening and crack closing. The development of a compressive stress field, which prevents further crack propagation, is one of the mechanisms of phase transformation that the model was able to explain before a crack tip. (Figure 3c) depicts the cracking process, however under the same temperature loading, silicon carbide has better deformation toughness than alumina and chromium carbide.

Studying the three ceramic materials' microcracking processes in (figure 3d) the performance of ceramics-based composite materials during fatigue in corrosive or high-temperature settings is the main area of interest. Phase transition and crack propagation interact significantly when subjected to heat stress, which was explored by Zhao and Mamivand [34, 36, 37] using PF modeling. However, this study demonstrates that compared to alumina and chromium carbide, silicon carbide has a higher factor of safety. In comparison to chromium carbide and alumina, which have respective minimum safety factors of 0.42729 and 0.064329, silicon carbide has a factor of safety of 2.8125. Additionally, it was noted that silicon carbide had a few small, isolated cracks on the geometry's surfaces (figure 3c), with the shear stress reaching its greatest value at 1700^0C.

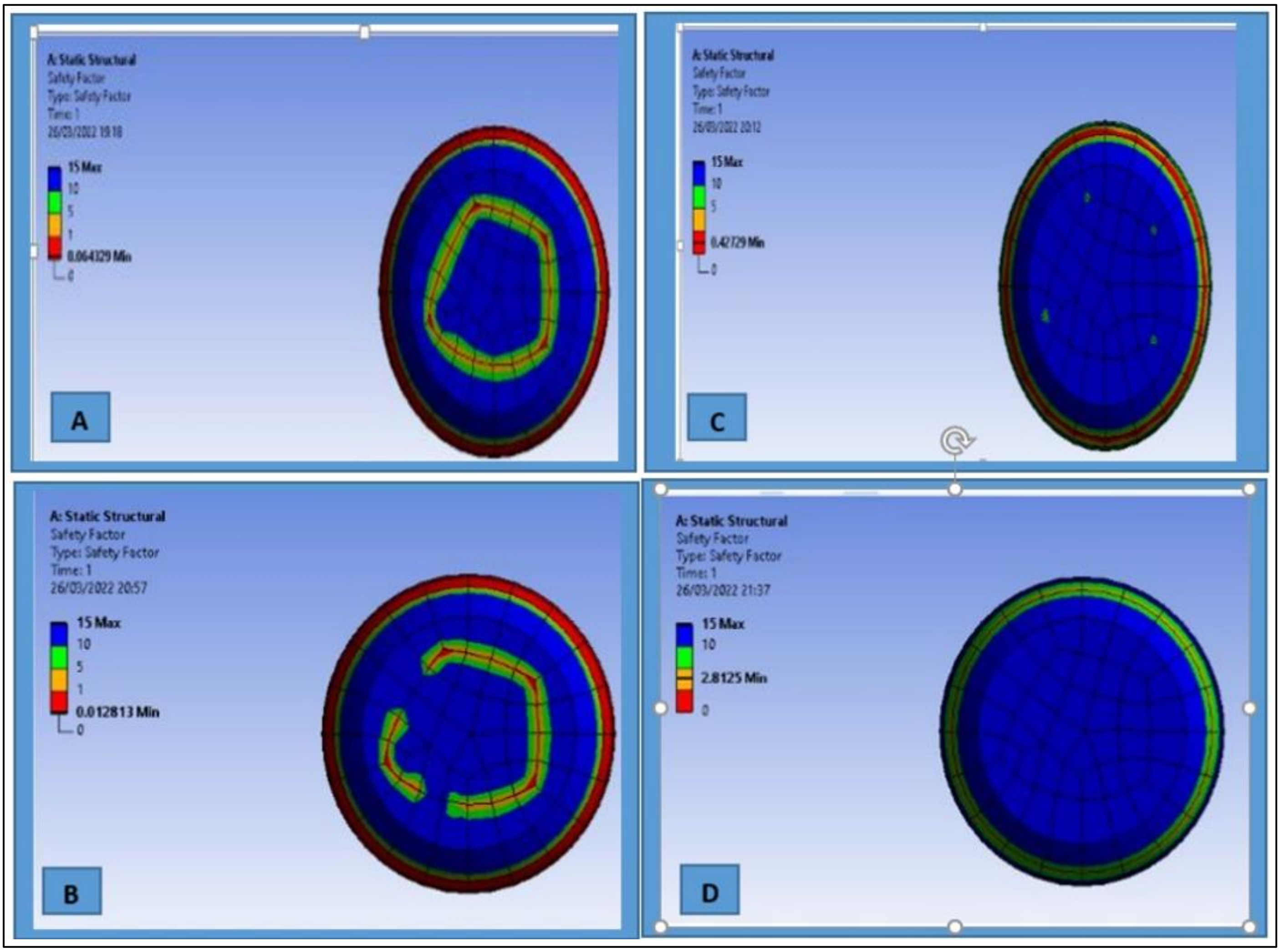

Fig 3 Meshing of Geometry Showing Deformation Under Varying Temperature Load. Microcracks Development: (a) Alumina at 1650^0C; (b) Chromium Carbide 1700^0C; (c)Silicon Carbide 1700^0C; (d) Silicon Carbide 1500^0

From the geometry, it was also possible to anticipate the spatial temperature and shear stress distribution immediately below melting point during the solid phase with respect to time (Figure 4). Figure 4a shows the distribution of shear stress for alumina ceramic-based materials at 1700 °C, with maximum and minimum values of 2.223 x 1010 and 9.476 x

ISSN No:-2456-2165 https://doi.org/10.38124/ijisrt/26sep160

108, respectively. Additionally, the center of the geometry exhibits higher shear stress than the edges, which gradually decreases toward the center, leading to the development of cracking at the center as opposed to the edges of other geometries (Figures 4a, 4b, and 4d). Furthermore, due to superior heat conduction and a larger temperature gradient, the material developed thermal stresses that made the center of another shape stronger than the edges. According to the findings, chromium carbide has maximum and minimum shear stresses of 7.0587 x 10-9 and 4.52279 x 10-8, respectively. Thermal stress was also shown to significantly increase at the geometry's outer edge region. This happened as a result of temperature differences, thermal expansion, and restrictions on the body's ability to expand and contract naturally. The anticipated thermal stresses for alumina, silicon carbide, and chromium carbide at the temperature range (between 800^0C and$1800^0\boldsymbol{C}$) are less than the flexural strength of alumina at 395 MPa, which is a crucial point to make.

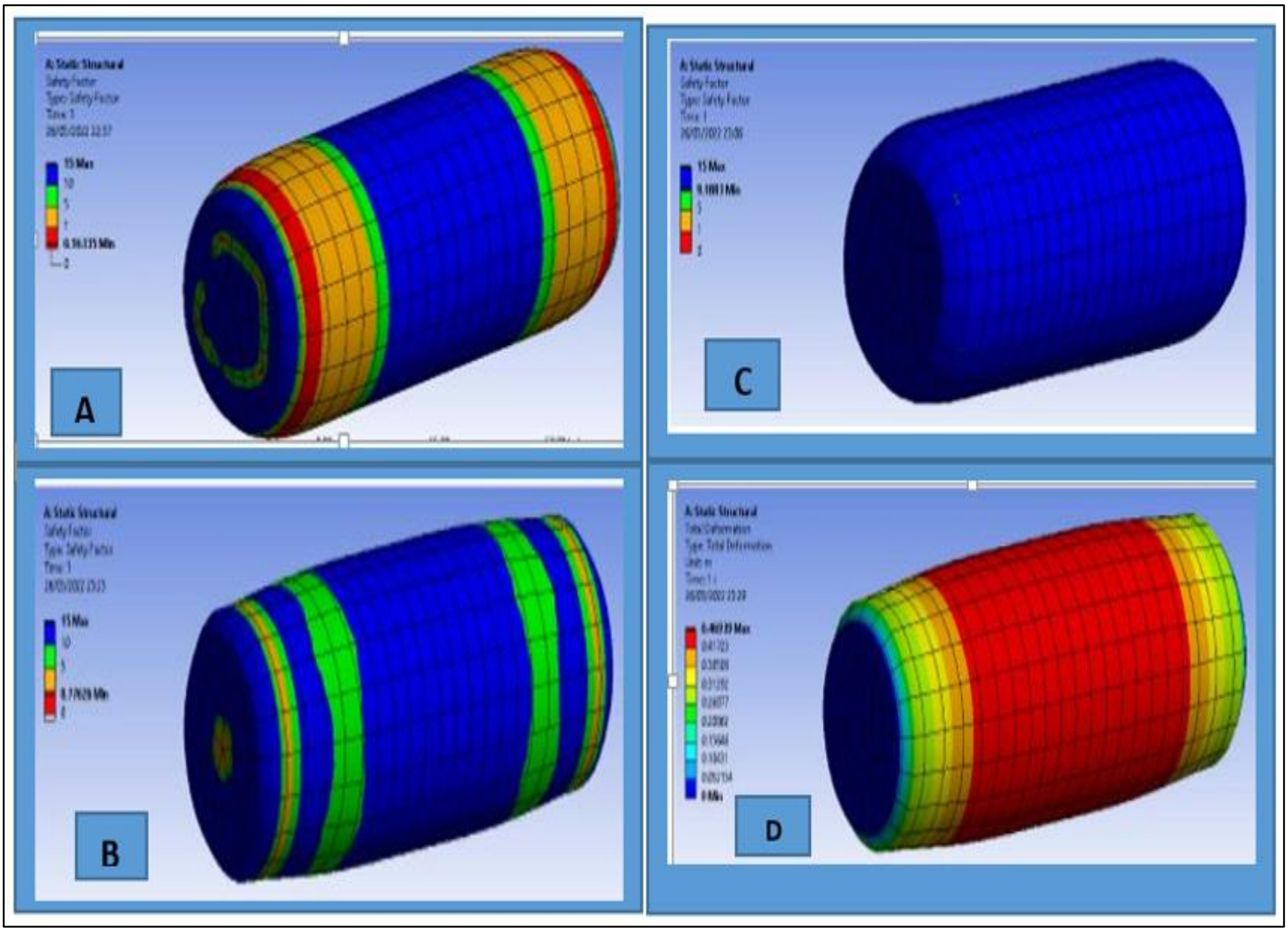

Fig 4 Stress-Strain Analysis Under Varying Thermal Conditions at 1700^0C; (a) Alumina 1700^0C; (b) Chromium Carbide (c) Silicon Carbide (d) Alumina at 1650^0C;

However, a multistep computational model developed for various ceramic-based materials at thermal condition magnitude was able to predict total deformation vs temperature (figure 5) as a function of time (t) from the boundary conditions set out at various thermal condition magnitude (800^0C, 1000^0C, 1400^0C, 1600^0C, and 1800^0C). As was previously mentioned, the optimization analysis solely took into account the solid phase thermal stresses as determined by computing. The thermal strain result at the peak temperature (Figure 6) and associated time period demonstrates that Alumina has a thermal strain of 0.0237 m/m, Silicon carbide has 0.0103 m/m, and Chromium carbide has 0.0124 m/m. This suggests silicon carbide has the lowest thermal strain compared to the other materials. Additionally, it is seen in (Figure 7) that the stresses were high on the surface and significantly decreased. The stresses on the surface thus grew near to the alumina's flexural strength with the potential for greater deformation and fracture production, according to both surface and depth profiles (figure 5).

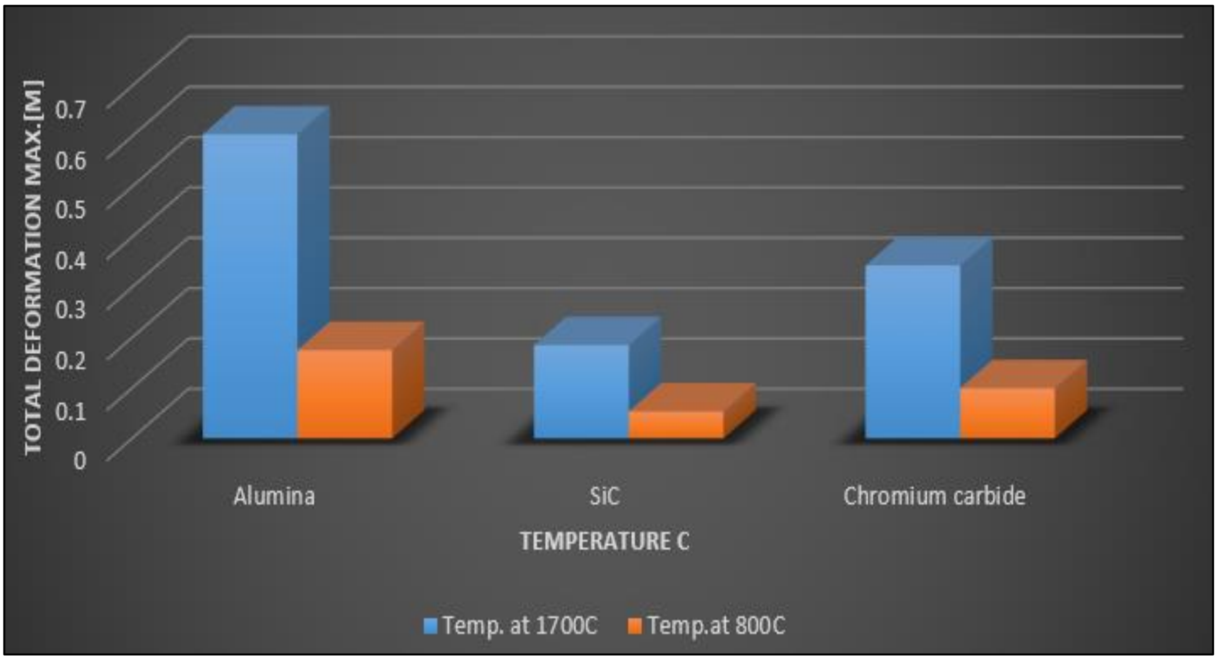

Fig 5 Total Deformation of the Three Ceramic Base Composite Materials against the Temperature Load.

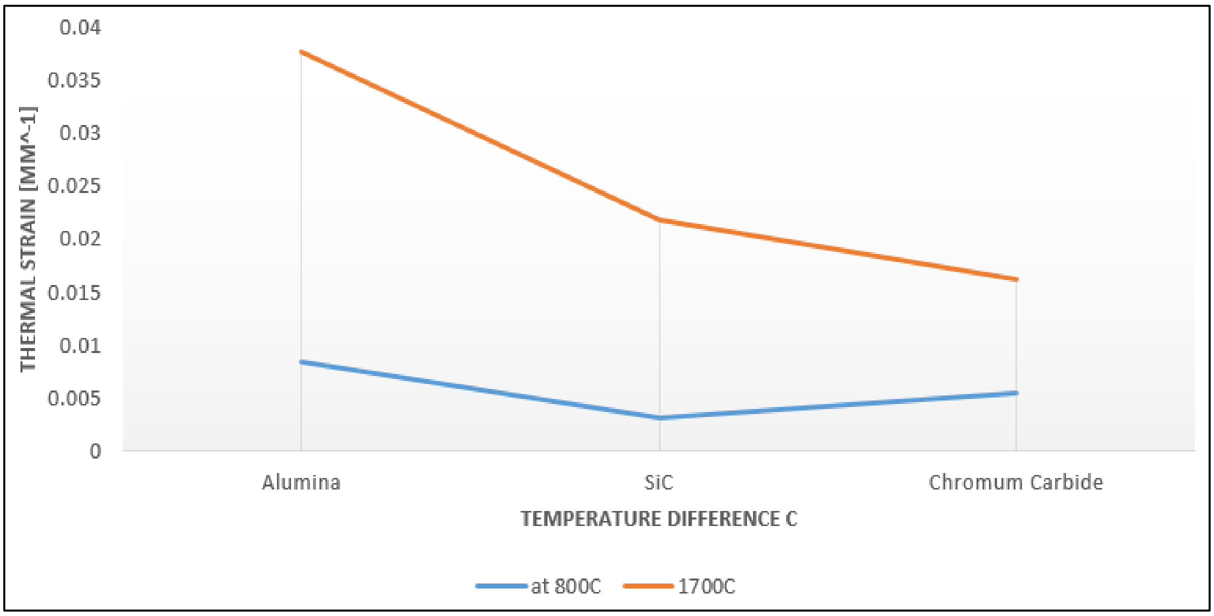

Fig 6 Thermal Strain of the Three Ceramic Base Composite Materials against the Temperature Difference.

Figure 3 shows the impact of growth and the safety factor on the rupture moduli of the three geometries more clearly, and Figure 6 shows the effects of thermal strain on the geometry as a function of temperature. The impact of temperature was more noticeable than the impact of time. When the temperature was increased from 1400° C to 1500° C, it was seen that the thermal stress of alumina was significantly lower than that of other materials. Above 1500°C, however, the joint strength declined. The maximum major elastic strain for alumina, which is prone to rupture, was 7.3954x106Pa at 1700 oC, while silicon carbide dissipated the least amount of elastic strain at 5.888x108Pa. The straightforward indicator of rupture demonstrates that the reaction zone's thickness is increasing with time and may ultimately determine the final strength of ceramic materials.

ISSN No:-2456-2165 https://doi.org/10.38124/ijisrt/26sep160

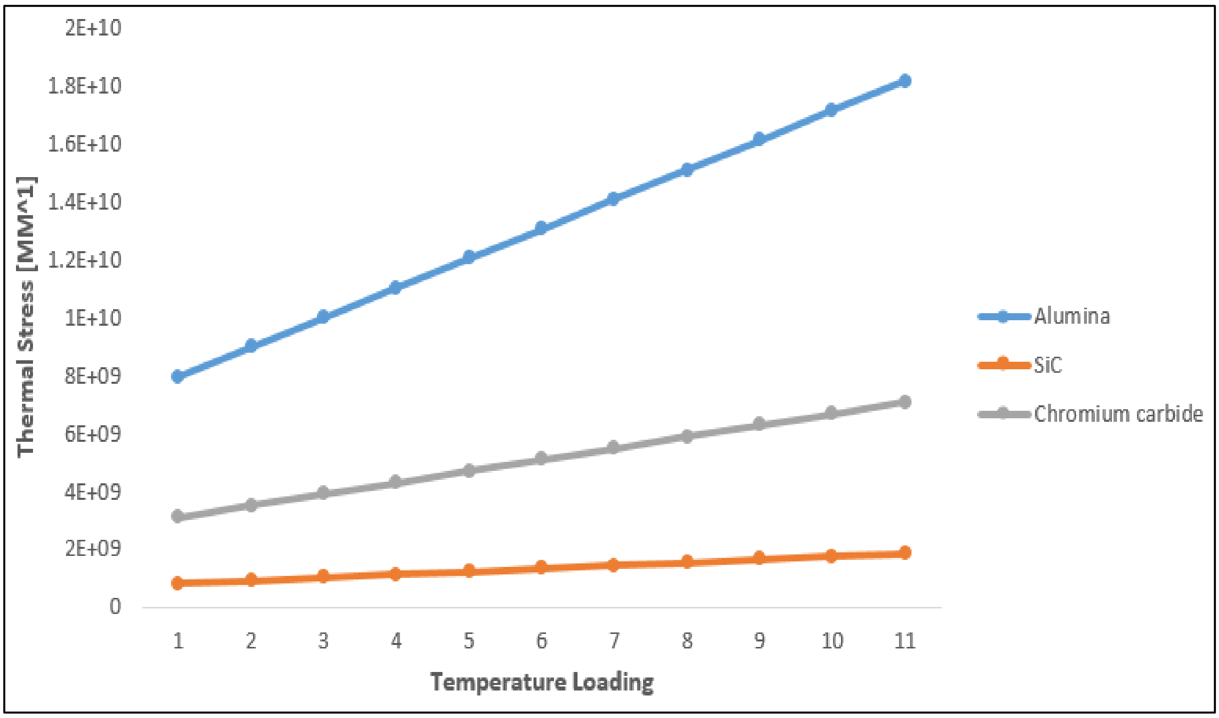

Fig 7 Thermal Stress of the Three Ceramic Base Composite Materials against the Temperature Loading.

IV. CONCLUSION

By varying the temperature range and examining the mechanical properties, the model's optimization has been carried out in this research project. Three ceramic materials' geometric properties—Alumina, Silicon Carbide, and Chromium Carbide were modeled and examined. Three ceramic materials' sensitivity to the microcracking process were examined. The different inferences made from the research include:

- It was observed that the cracking process advances uniformly into the interfaces system in all the three ceramic materials optimised. In addition to compressive stress field, stresses also initiate cracking through phase deformation

- The research demonstrates that silicon carbide is safer than alumina and chromium carbide at temperature of 1750^0C. Compared to chromium carbide and alumina, which have minimal safety factors of 0.42729 and 0.064329, respectively, silicon carbide has a factor of safety of 2.8125.

- Thermal strain testing revealed that at 1800^0C, Alumina had a thermal strain of 0.0237 m/m, Silicon carbide had 0.0103 m/m, and Chromium carbide had 0.0124 m/m. According to this, silicon carbide has lower thermal stress than the other materials.

- Silicon carbide dissipates elastic strain at a minimum of 5.888x108Pa. The straightforward indicator of rupture demonstrates that the reaction zone's thickness is increasing with time and may ultimately determine the strength of ceramic materials.

- Hence, the efficiency and thermal characteristics of ceramic composite materials have thus been optimized. According to the aforementioned findings, silicon carbide's compressive stress field displayed greater thermal strength than alumina and chromium carbide at temperatures higher than 1800^0C.

ACKNOWLEDGMENTS

The authors gratefully acknowledge the support of Department of Mechanical Engineering, University of Ibadan, Ibadan, Nigeria. And Advanced Aerospace Engine Laboratory Oka Akoko, Ondo, Nigeria for granting access to their laboratory.

➢ *Author Contributions*

- C. Ogundola: Data curation, Formal Analysis, Investigation, Methodology, Software, Validation, Visualization, Writing – original draft
- O. O. Ajide: Conceptualization, Project administration, Resources, Supervision, Writing – review & editing
- T. E. Omoniyi: Data curation, Software, Validation, Supervision
- E. T. Daodu: Investigation, Software, Visualization, Writing – original draft
- O. Alake: Software, Formal Analysis, Visualization
- J. O. Ikare: Formal Analysis, Investigation, Project administration
- S. O. Olowo: Data curation, Software, Writing – original draft
- O. P. Aminu: Data curation, Validation, Project administration

➢ *Data Availability Statement*

All data generated or analyzed during this study are included in this article.

➢ *Conflicts of Interest*

The author declares no conflict of interest.

REFERENCES

[1]. J. Moqdad, S. Nabaa, Radh, Manar A, S. Zainab (2021) "Optimization of Electro less of Nickel base coating for Cermet Cutting Tools Substrate" Journal of Mechanical Engineering Research and Developments ISSN: 1024-1752

[2]. Tingrui Gong, Feng Qin, Xinzhu Yan, Lei Gao, Yingkun Yang, Zhicheng Lei, Haoshu Tan and Juntao Li (2022) "Thermo-Mechanical Optimization of Ceramic Substrate with through Ceramic vias by Taguchi-Grey Method" Microelectronics Reliability Volume 132, May 2022, 114535 https://doi.org/10.1016/j.microrel.2022.114535

[3]. R. Rico, J. Irene, and B. Eckhard, (2012) "Optimization of the aluminum oxide properties for adhesive bonding by laser surface pretreatment" Journal of Laser Applications 24, 032002 (2012); doi: 10.2351/1.4704854

[4]. L. Song, Y. Dong, Q. Shao, and J. Jiang, "Synthesis of monodisperse α- Al2O3 nanoparticles by a salt microemulsion method," Micro Nano Letter, vol. 13, no. 8, pp. 1071–1074, 2018, doi:10.1049/mnl.2018.0078

[5]. Z. Adzra, K. Yuni, S. Yusrianti, R. Risti, B. Asep, Tedi K., (2021) :Recent Progress on the Production of Aluminum Oxide (Al2O3) Nanoparticles: A Review. Mechanical Engineering for Society and Industry, Vol.1 No.2 (2021). https://doi.org/10.31603/mesi.5493

[6]. U. A. Usca, M. Uzun, M. Kuntoglu, E. Sap, MK. Gupta. Investigations on Tool Wear, Surface Roughness, Cutting Temperature, and Chip Formation in Machining of Cu-B-CrC composites. Int J Adv Manuf Technol 2021;116(9):3011e25

[7]. S. Agarwal, PV. Rao (2013) Predictive modeling of force and power based on a new analytical undeformed chip thickness model in ceramic grinding. Int J Mach Tools Manuf 65:68–78 alumina nanoparticles using some plants extracts," Journal of Nanostructures, vol. 7, no. 1,

[8]. M. Uzun, and MS. Etin. Investigation of Characteristics of Cu based, Co-CrC Reinforced Composites Produced by Powder Metallurgy Method. Adv Powder Technol 2021;32(6):1992e2003

[9]. B. Zhang, XL. Zheng, H. Tokura, M. Yoshikawa (2003) Grinding induced damage in ceramics. J Mater Process Technol 132(1–3):353–364

[10]. E. Sap. (2021) Investigation of Mechanical Properties of Cu/Mo-SiCp Composites Produced with P/M, and their Wear behavior with the Taguchi method. Ceram Int 2021;47(18):25910e20

[11]. S. Agarwal, PV. Rao (2008) Experimental investigation of surface/ subsurface damage formation and material removal mechanisms in SiC grinding. Int J Mach Tools Manuf 48(6):698–710

[12]. TJ. Holmquist , GR. Johnson(2005) Characterization and evaluation of silicon carbide for high-velocity impact. J Appl Phys 97(9): 093502.1–093502.12

[13]. S. Wei, H. Zhao, J. Jing, Y. Liu (2015) Investigation on surface microcrack evaluation of engineering ceramics by rotary ultrasonic grinding machining. Int J Adv Manuf Technol 81:483–492

[14]. S. Sharma, Singh Jujhar, Gupta Munish Kumar, Mia Mozammel, Dwivedi Shashi Prakash and Saxena Ambuj. (2021) "Investigation on mechanical, tribological and microstructural properties of AleMgeSieT6/SiC/muscovitehybrid metal-matrix composites for high strength applications". J Mater Res Technol 2021;12:1564e81

[15]. M. Chen, Q. Zhao, S. Dong, Li D (2005) The critical conditions of brittle–ductile transition and the factors influencing the surface quality of brittle materials in ultra-precision grinding. J Mater Process Technol 168(1):75–82.7 Collection, vol. 29, p. 100531, 2020, doi: 10.1016/j.cdc.2020.100531.

[16]. A. Kurzawa., J.W. Kaczmar, Bending strength of composite materials with EN AC-44200 matrix reinforced with Al2O3 particles, Archives of Foundry Engineering. 15 (2015) 61–64.

[17]. S. Hutzler., R. John., F. Friedrich., W. Denis (2018): A simple formula for the estimation of surface tension from two length measurements for a sessile or pendant drop. Philosophical Magazine Letters 98(1):1-8 DOI:10.1080/09500839.2018.1434320

[18]. E. Salur, A. Aslan, M. Kuntoglu, M. Acarer (2021) "Effect of Ball Milling Time on the Structural Characteristics and Mechanical Properties of Nano-Sized Y2O3 Particle Reinforced Aluminum Matrix Composites Produced by Powder Metallurgy Route". Adv Powder Technol 2021;32(10):3826e44

[19]. J. Timothy Holmquista and Gordon R. Johnson (2005) "Characterization and evaluation of silicon carbide for high-velocity impact" Journal of Applied Physics 97, 093502 (2005); doi: 10.1063/1.1881798

[20]. L. Krüger, K. Mandel, R. Krause and Radajewski M 2015 Int. J. Refrac. Met. Hard. Mat. 51 324–31

[21]. Huang Z Q and Gang L 2017 Eng. Fail. Anal. 80 273-77

[22]. E. Postek and T. Sadowsk (20018) "Impact Modelling of Cermet Composites" IOP Conf. Series: Materials Science and Engineering 416 (2018) 012088 doi:10.1088/1757-899X/416/1/012088

[23]. NS. Ross, et al. (2022) "Impact of Hybrid Cooling Approach on Milling and Surface Morphological Characteristics of Nimonic 80A Alloy". J Manuf Process 2022;73:428e39.

[24]. H. Dębski and T. Sadowski 2014 Comput. Mat. Sci. 83 403-11

[25]. H. Dębski and T Sadowski 2017 Comp. Struct. 159 121-2

[26]. Yathish Narayana Rao and Mohamed Kaleemulla K (2018) Mechanical Properties of Pure [27] Aluminum Oxide . internation Journal of Mechanical and

Production Engineering Research and Development 8(2):355-362 DOI:10.24247/ijmperedapr201839

[27]. R. Pandiyarajan, M.P Prabakaran, Vetrivel Kumar, Rajkumar and Manikandan R (2021) "Metallurgical and mechanical properties of SiC/B_4 C reinforced with aluminum composites synthesized by mechanical alloying" Materials Today: Proceedings Volume 37, part 2, DOI.org/10.1016/j.matpr.2020.07.397

[28]. X. Zeng, A. Lai, C.L. Gan, C.A. Schuh, (2016) Crystal orientation dependence of the stress-induced martensitic transformation in zirconia-based shape memory ceramics, Acta Mater. 116 (2016) 124–135

[29]. T. Sadowski and P. Trovalusci (Eds) (2014) Multiscale Modelling of of Complex Materials, CISM Courses and Lectures No. 556 International Centre for Mechanical Sciences (Wien –NewYork: Springer

[30]. L.M. Kachanov (1986) Introduction to Continuum Damage Mechanics (Dordrecht: Martinun Nijhoff Publishers)

[31]. M. Ferraiuolo,.; C. Palumbo,.; A. Sellitto.; A Riccio, (2020) "Global/Local Finite Element Analyses Supporting The Design Of A Ceramic Matrix Composite Wing Leading Edge Of A Re-Entry Vehicle". Mater. Today Proc. 2020.

[32]. P. P. Camanhi and C. G. Davila (2002) Mixed-Mode Decohesion Finite Elements for the Simulation of Delamination in Composite Materials NASA/TM-2002-211737

[33]. M. Mamivand, M. Asle Zaeem, H. El Kadiri, (2014) Phase field modeling of stress-induced-tetragonal-to-monoclinic transformation in zirconia and its effect on transformation toughening, Acta Mater. 64 (2014) 208–219

[34]. P. Gosselet,; M. Blanchard.; O. Allix,; G. Guguin, . (2020) "Non-invasive Global–Local Coupling as a Schwarz Domain Decomposition Method: Acceleration and Generalization". Adv. Model. Simul. Eng. Sci. 2018,

[35]. T. Zhao, J. Zhu, J. Luo, (2016) Study of crack propagation behavior in single crystalline tetragonal zirconia with the phase field method, Eng. Fract. Mech. 159 (2016) 155–173

[36]. MK. Gupta, M. Boy, ME. Korkmaz, N. Yas,ar, Gu¨ nay M, GM. Krolczyk. (2022) "Measurement and Analysis of Machining Induced Tribological Characteristics in dual Jet Minimum Quantity Lubrication Assisted Turning of Duplex Stainless Steel Measurement" 2022;187:110353